

Diffraction of x rays at the far tails of the Bragg peaks

Ariel Caticha*

*National Institute of Standards and Technology, Gaithersburg, Maryland 20899
and Institute for Physical Science and Technology, University of Maryland, College Park, Maryland 20742*

(Received 21 May 1992)

It is known that the kinematical and dynamical theories of diffraction by perfect crystals predict the same values for the intensities scattered into the vicinity of the Bragg peaks whenever those intensities are low. Here we address the question of whether this is also true throughout the region between two Bragg peaks. We show that the two theories give equivalent results for the weak intensities in the far tails of the Bragg peaks provided better approximations for both the shape of the dispersion surface and the boundary conditions are used: One needs to take into account the asymptotic sphericity of the dispersion surface and the difference between electric and displacement fields. This results in a nontrivial transmission coefficient for the diffracted electric field as it leaves the crystal. By explicitly showing the equivalence of kinematical and dynamical results, this work provides additional theoretical support for the kinematical approach usually adopted to describe the so-called truncation-rod scattering.

I. INTRODUCTION

The theories traditionally used to study the scattering of x rays by crystals are usually referred to as being either kinematical or dynamical theories of diffraction.¹⁻⁴ The former group of theories is based on the premise that if the scattered intensity is low, then a single scattering or first Born approximation should be accurate. The kinematical theories may therefore fail at the Bragg peaks where high scattered intensities are not uncommon. This limitation is overcome in the dynamical theories by explicitly taking multiple scattering into account. The basic assumption made in these theories is that the dielectric susceptibility $\chi(\mathbf{r})$ of the crystal is very small (about 10^{-5}) and this allows one to make various simplifying approximations. The most important consists of neglecting all but a finite number n of the diffracted beams; this reduces the problem to a practically manageable size. But other simplifications are routinely made such as neglecting terms of order χ^2 , using approximate forms of the boundary conditions, and restricting oneself to the close vicinity of the Bragg peaks, to name a few. Thus, various *modified* dynamical theories have emerged to treat the special cases where one or other of those approximations fail, such as, for example, for grazing incidence when the reflection by the crystal surface is not negligible,⁵ or for Bragg angles close to $\pi/2$ when more accurate forms of the dispersion surface have to be considered.⁶

It is widely believed that whenever the scattered intensities are low the kinematical and dynamical theories of diffraction give the same results. This has been shown to be the case when either the Bragg reflection is very weak or when the crystal is sufficiently thin, but only in the close vicinity of the Bragg peaks. The question of whether this is still true throughout the region between two Bragg peaks has not been addressed. In fact, several approximations of the dynamical theory fail in this region and they have to be appropriately corrected.

The purpose of this paper is to develop improved approximations to the dynamical diffraction theory in order to describe accurately the far tails of the Bragg peaks. We find that it is necessary to take into account the correct asymptotic sphericity of the dispersion surface and the correct electromagnetic boundary conditions. The expected agreement between the reflectivities according to the kinematical and the presently modified dynamical theory is obtained, but the way in which this comes about is quite unexpected. In fact, the kinematical and dynamical descriptions of the diffracted fields within the crystal are so different that the eventual agreement is actually rather surprising.

The interest in the study of the diffraction in the far tails of the Bragg peaks is not purely academic. One possible practical application is in the so-called truncation-rod scattering (TRS).⁷ Modern x-ray-scattering techniques allow the measurement of the scattered intensity from just a few layers of atoms. This has led to new methods for the study of surfaces based on the idea that if the intensity scattered from an ideal crystal with an ideal surface is known, then any observed deviations can lead to information about the structure either of the bulk or of the surface. In the vicinity of the Bragg peaks the waves scattered from different bulk atoms interfere constructively leading to large diffracted intensities that prevent the observation of the small contribution of the surface atoms. Thus, in order to observe the scattering from the surface atoms with the least possible bulk interference one has to go far away (perhaps a degree or more) from the Bragg peaks. These studies have traditionally been carried out using the framework of the kinematical theory of x-ray diffraction,⁷ which is justified, correctly if somewhat vaguely, by the small scattered intensities.

The statement that the kinematical theory is valid whenever the reflectivity is low is a very valuable rule of thumb, of very wide applicability, but it is not universally valid. Known examples of its failure include x-ray diffraction by multilayered structures⁸ and the scattering

by surfaces at grazing incidence for which corrections to the kinematical theory, which go under the name of the distorted-wave approximation, are required.⁹ Thus, while there is no reason to doubt the validity of the kinematical treatment adopted in Ref. 7, an alternative dynamical treatment may be of value. In a recent contribution, Colella¹⁰ has shown that some of the basic features of TRS can be reproduced by the dynamical theory. He used a numerical approach that avoids most, but not all, of the approximations normally made in the dynamical theory (this is still an n -beam calculation with finite n , and one has to consider which is the best set of n beams to be included in the calculation). He showed that if one scans reciprocal space in a direction transverse to the kinematical truncation rods the dynamical theory predicts a peak at roughly the same position as the kinematical theory. The question of whether the dynamical intensities are in numerical agreement with the kinematical ones was not, however, addressed.

A second situation where the modified dynamical theory described here will find application is in the diffraction of x rays by periodic multilayered structures⁸ at low Bragg angles. In this regime many Bragg peaks are crowded close together, and one does not have to go very far away from the peaks in order to reach the far tails where the usual approximations fail. Both applications will be studied in more detail elsewhere.

In order to establish the notation and define the problem we calculate, in Sec. II, the reflectivity of a crystal according to a kinematical theory that includes the effects of absorption, index of refraction, and of the Fresnel reflectivity. The same reflectivity is then calculated according to the usual Laue dynamical theory drawing attention to the various approximations made. The two results are compared in the case of CuK α diffraction by the (111) planes of a silicon crystal and found to disagree appreciably in the far tail region. The various improvements of the dynamical theory required to bring about agreement with the kinematical theory are discussed in Sec. III. In order to avoid complications that would unnecessarily obscure the issues at hand, we have focused our attention mainly on the special case of diffraction of TE polarized radiation by a semi-infinite crystal with an idealized abruptly terminated surface. Some of the expressions below are, however, of more general validity. In Sec. IV, we summarize our conclusions.

II. A DISAGREEMENT BETWEEN THE KINEMATICAL AND THE DYNAMICAL THEORIES

A. A kinematical diffraction theory

Consider a crystal slab with plane parallel surfaces, thickness L , and dielectric susceptibility

$$\chi(\mathbf{r}) = \sum_H \chi_H e^{i\mathbf{H}\cdot\mathbf{r}}, \quad (2.1)$$

where \mathbf{H} are the reciprocal lattice vectors. The use of such a highly idealized mathematical model with ideally abrupt surfaces at $z=0$ and $z=L$ (see Fig. 1) is justified because it provides a simple testing ground for the ap-

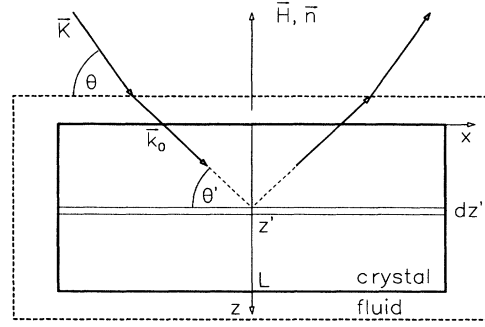


FIG. 1. Geometry of kinematical diffraction in the symmetric Bragg case.

proximations involved in the various diffraction theories (and not because it is a realistic model of surface structure).

For symmetric Bragg case diffraction (Fig. 1) we need to consider only those \mathbf{H} vectors lying along the z direction, which are those on the truncation rod passing through the origin in reciprocal space. Let us first neglect the effects of absorption and refraction. According to the Fresnel diffraction theory^{4,11} an incident plane wave $\mathbf{E}_0 e^{i\mathbf{k}_0\cdot\mathbf{r}}$ is scattered by a layer of matter of susceptibility $\chi(z')$, thickness dz' and located at depth z' into the crystal into a plane wave of wave vector \mathbf{k} given by

$$\delta\mathbf{E}(z') = \frac{-iK}{2 \sin\theta'} e^{2ik_{0z}z'} \chi(z') dz' \hat{\mathbf{k}} \times (\hat{\mathbf{k}} \times \mathbf{E}_0) e^{i\mathbf{k}\cdot\mathbf{r}}, \quad (2.2)$$

where $K = \omega/c$ and the wave vector \mathbf{k} is obtained from the incident \mathbf{k}_0 by specular reflection:

$$|\mathbf{k}| = |\mathbf{k}_0|, \quad \text{and } k_z = -k_{0z}. \quad (2.3)$$

The total electric field scattered by the crystal is obtained by integrating in z' from 0 to L and the reflectivity is given by the ratio $|E|^2/|E_0|^2$:

$$R_K = \left| \frac{P}{4 \sin\theta'} \sum_H \chi_H \frac{e^{2iKL(\sin\theta' - \sin\theta_H)} - 1}{\sin\theta' - \sin\theta_H} \right|^2, \quad (2.4)$$

where θ_H is the Bragg angle corresponding to the vector \mathbf{H} , θ' is the angle of incidence within the crystal, and the factor P is 1 or approximately $\cos 2\theta$ for TE or TM polarization, respectively. Expressions similar to (2.4) have been routinely used in surface diffraction studies.⁷

Let us now include the effects of absorption and refraction. These effects may be disentangled from those of diffraction if we imagine the crystal immersed in an amorphous fluid (see Fig. 1) with susceptibility equal to the average susceptibility of the crystal [χ_0 in Eq. (2.1)]. The wave vector \mathbf{K} incident on the external vacuum-fluid surface is refracted into the (possibly complex) wave vector \mathbf{k}_0 , which is continuous across the fluid-crystal surface. After calculating the scattered intensity we may take the limit of vanishing fluid volume. Thus, refraction and absorption effects are described by letting

$$\mathbf{k}_0 = \mathbf{K} + K \Delta_K \hat{\mathbf{n}}, \quad (2.5)$$

where

$$\Delta_K = \sin\theta - \sin\bar{\theta}$$

and

$$\sin\bar{\theta} \equiv (\sin^2\theta + \chi_0)^{1/2}.$$

The steps leading to (2.2) and (2.4) may be repeated. The result is an expression for the reflectivity that is identical to (2.4) except that $\sin\theta'$ is replaced by the complex quantity $\sin\bar{\theta}$ and there is an irrelevant extra factor of $|1 + \chi_0|^2 \approx 1$. For future reference, for a semi-infinite crystal we get

$$R_K = \left| \frac{P}{4 \sin\bar{\theta}} \sum_H \frac{\chi_H}{\sin\theta_H - \sin\bar{\theta}} \right|^2. \quad (2.6)$$

This expression is accurate everywhere except very close to the Bragg peaks, where $\sin\theta_H \approx \sin\bar{\theta}$ and R_K is large. In particular, (2.6) fails at grazing incidence where total reflection (the zeroth-order Bragg peak) occurs. This may be corrected by replacing the $H=0$ term by the correct Fresnel reflection coefficient,

$$R_K = \left| r_F + \frac{P}{4 \sin\bar{\theta}} \sum_{H \neq 0} \frac{\chi_H}{\sin\theta_H - \sin\bar{\theta}} \right|^2, \quad (2.7)$$

where

$$r_F^{\text{TE}} = \frac{\sin\theta - \sin\bar{\theta}}{\sin\theta + \sin\bar{\theta}} \quad (2.8)$$

or

$$r_F^{\text{TM}} = \frac{(1 + \chi_0)\sin\theta - \sin\bar{\theta}}{(1 + \chi_0)\sin\theta + \sin\bar{\theta}}, \quad (2.9)$$

for TE or TM polarizations, respectively.

B. The usual Laue dynamical diffraction theory

Laue's approach to the dynamical diffraction theory consists in solving Maxwell's equations in a periodic medium described by the susceptibility (2.1) and matching this internal solution to external vacuum fields through appropriate boundary conditions. In the two-beam approximation,¹⁻³ the displacement field within the crystal is a Bloch wave of the form

$$\mathbf{D}(t, \mathbf{r}) \simeq e^{-i\omega t} (\mathbf{D}_0 e^{i\mathbf{k}_0 \cdot \mathbf{r}} + \mathbf{D}_H e^{i\mathbf{k}_H \cdot \mathbf{r}}), \quad (2.10)$$

where $\mathbf{k}_H = \mathbf{k}_0 + \mathbf{H}$ and the amplitudes satisfy the system of equations

$$2\xi_0 D_0 - P\chi_{-H} D_H = 0, \quad (2.11a)$$

$$-P\chi_H D_0 + 2\xi_H D_H = 0, \quad (2.11b)$$

with the resonance defects ξ_0 and ξ_H defined by

$$\xi_0 = \frac{\mathbf{k}_0^2 - K^2(1 + \chi_0)}{2\mathbf{k}_0^2}, \quad (2.12a)$$

$$\xi_H = \frac{\mathbf{k}_H^2 - K^2(1 + \chi_0)}{2\mathbf{k}_H^2}. \quad (2.12b)$$

The wave vectors \mathbf{k}_0 and \mathbf{k}_H are determined by two conditions: The first is that they are constrained to lie on the dispersion surface. This is expressed by

$$\xi_0 \xi_H = \frac{1}{4} P^2 x^2, \quad (2.13)$$

where $x^2 \equiv \chi_H \chi_{-H}$ and P is the polarization factor. As shown in Fig. 2, this consists of two spheres centered at 0 and H and deformed at their intersection, which is where the Bragg peak occurs. The second is that they are related to the incident vacuum wave vector \mathbf{K} through a tangential continuity boundary condition analogous to (2.5)

$$\mathbf{k}_0 = \mathbf{K} + K \Delta \hat{\mathbf{n}}. \quad (2.14)$$

Only two approximations have been made so far: We have neglected terms of order χ^2 and have restricted ourselves to only two beams. Now we make two additional approximations that are central to the discussion in this paper: First we assume that the resonant defects are small quantities,

$$\xi_0, \xi_H \approx \mathcal{O}(\chi), \quad (2.15)$$

the square of which may be safely neglected. This approximation is very good close to the Bragg peaks but fails otherwise. Equations (2.12) then simplify to

$$k_0^2 = K^2(1 + \chi_0 + 2\xi_0), \quad (2.16a)$$

$$\mathbf{k}_H^2 = K^2(1 + \chi_0 + 2\xi_H). \quad (2.16b)$$

The second is to assume that Δ is small,

$$\Delta \approx \mathcal{O}(\chi), \quad (2.17)$$

and its square is negligible. This is a good approximation except at grazing incidence where Δ is of order $\chi^{1/2}$. For the sake of simplicity in the rest of this section we will restrict ourselves to the TE polarization ($P=1$) and the symmetric Bragg case ($\hat{\mathbf{n}} = \mathbf{H}/H$). This is sufficient for our present purposes. Equations (2.13)–(2.17) then imply

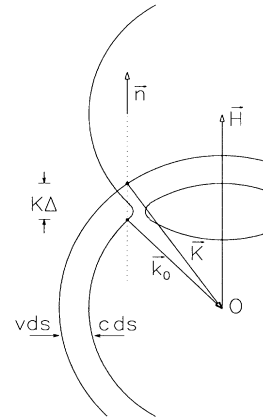


FIG. 2. The dispersion surface in the crystal (cds) in the two-beam case and in vacuum (vds). The surface normal $\hat{\mathbf{n}}$ and the wave vectors in vacuum \mathbf{K} and in the crystal \mathbf{k}_0 are related by Eq. (2.14).

$$\Delta = \frac{(1/2)\chi_0 + \xi_0}{\hat{\mathbf{n}} \cdot \hat{\mathbf{K}}} \quad (2.18)$$

and

$$\xi_0 = \frac{1}{2}[-z \pm (z^2 - x^2)^{1/2}], \quad (2.19)$$

where

$$z = \chi_0 - a$$

and

$$a = \frac{2\mathbf{K} \cdot \mathbf{H} + H^2}{2K^2} = 2 \sin\theta_H (\sin\theta_H - \sin\theta). \quad (2.20)$$

Equations (2.18) and (2.19) amount to approximating the dispersion surface (2.13) by a hyperboloid with straight rather than curved asymptotes. It is also usual¹⁻³ to approximate the incidence variable a by expanding the right-hand side of (2.20) to first order in $\delta\theta = \theta - \theta_H$. This is obviously wrong far from the Bragg peaks.

The last ingredient in the calculation of the reflectivity consists of matching the fields within the crystal to those outside. The fact that χ is small allows one to neglect the distinction between the electric (E) and the displacement (D) fields and to replace the exact electromagnetic boundary conditions of continuity of the appropriate tangential or normal component of a field by the continuity of its amplitude. For a semi-infinite crystal the amplitude of the diffracted field in vacuum is then given by the Bloch wave amplitude ratio

$$r_A = \frac{D_H}{D_0} = \frac{2\xi_0}{\chi - H}, \quad (2.21)$$

with the sign of Eq. (2.19) chosen to minimize $|r_A|^2$. The dynamical reflectivity, corresponding to the kinematical Eq. (2.7), is

$$R_{L1} = |r_F + r_A|^2. \quad (2.22)$$

In Sec. III we will see that the approximate boundary condition of continuity of the field amplitudes fails far from the Bragg peaks and Eq. (2.22) will have to be revised.

C. The kinematical and dynamical results compared

Let us consider the specific case of diffraction of TE-polarized $\text{CuK}\alpha$ radiation by the (111) planes of the ideally terminated semi-infinite silicon crystal. The reflectivity calculated according to the kinematical and Laue dynamical theories, given by Eqs. (2.7), (2.8), and (2.22), respectively is shown in Fig. 3. The close vicinity of the Bragg peak is shown in Fig. 3(a). We see that the kinematical (curve labeled KT) and dynamical (curve labeled LT1) results agree for low values of the reflectivity (say, for $R < 10^{-2}$), while the kinematical result is obviously wrong where R is large. This is well known. Note, incidentally, that the index of refraction correction included in the kinematical reflectivity of Eq. (2.7) provides the appropriate shift so that the location of the kinematical peak agrees with the dynamical one.

What is perhaps not as widely appreciated is that as

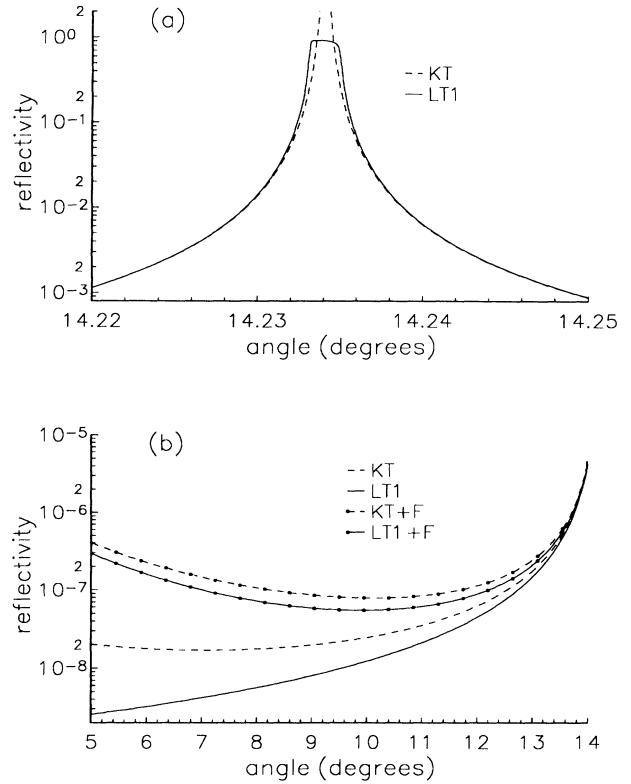


FIG. 3. (a) The reflectivity of the ideally terminated silicon crystal to $\text{CuK}\alpha$ radiation according to the kinematical (KT) and the usual Laue dynamical theories (LT1) in the vicinity of the (111) Bragg peak. (b) The same reflectivity in the far tail region with (curves labeled KT+F and LT1+F) and without (curves labeled KT and LT1) the contribution due to the Fresnel reflectivity.

one goes farther and farther from the Bragg peak the two theories give diverging results [Fig. 3(b)]. We see that the reflectivities without the contribution due to the Fresnel reflectivity (curves labeled KT and LT1, respectively), which are obtained from Eqs. (2.7) and (2.22) by omitting the r_F term, may differ by a factor of 10 or more. Of course, as one goes away from one Bragg peak the influence of the tails of neighboring ones becomes important. In this particular case the rather large contribution of the Fresnel reflectivity should be included (curves labeled KT+F and LT1+F) and we see that the disagreement is milder, but it still is large, of the order of 50%.

Let us now address the issue of whether the expectation that the kinematical and dynamical theories give the same results whenever the reflectivities are low is a natural one or not. Notice that quite independently of the issue of the validity of the approximations (2.15) and (2.17), the two theories necessarily give very different descriptions of the diffracted field within the crystal. The kinematical diffracted wave vector \mathbf{k} is related to the incident wave vector \mathbf{k}_0 by specular reflection, Eq. (2.3), while the dynamical wave vector \mathbf{k}_H is given by $\mathbf{k}_H = \mathbf{k}_0 + \mathbf{H}$. As shown in Fig. 4, close to the Bragg peak these two forms are approximately equal. In the far tail

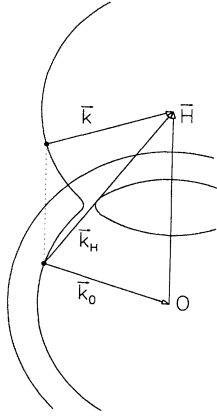


FIG. 4. The kinematical \mathbf{k} and the dynamical \mathbf{k}_H diffracted wave vectors. They are very different except close to the Bragg peak (the region in which the spheres intersect and the dispersion surface deviates from sphericity). \mathbf{k}_0 is the wave vector of the primary plane wave.

region, however, they are so different that any agreement between the dynamical and kinematical reflectivities would actually be rather surprising.

III. AN IMPROVED LAUE DYNAMICAL THEORY

A. The dispersion surface

In Sec. II C we saw that approximations (2.15) and (2.17), which amount to neglecting the asymptotic sphericity of the dispersion surface, are not valid in the far tail region. A quartic equation for the dispersion surface that is exact (within the approximations of keeping only two beams and neglecting χ^2) is obtained by eliminating ξ_0 and ξ_H from Eqs. (2.12)–(2.14). This leads to

$$\Delta^4 + C_3\Delta^3 + C_2\Delta^2 + C_1\Delta + C_0 = 0, \quad (3.1)$$

where

$$C_3 = 2\hat{\mathbf{n}} \cdot \hat{\mathbf{K}} \left[1 + \frac{1}{b} \right], \quad (3.2a)$$

$$C_2 = 2 \left[a + \frac{2}{b} (\hat{\mathbf{n}} \cdot \hat{\mathbf{K}})^2 - \frac{\chi_0 + x^2}{1 - x^2} \right], \quad (3.2b)$$

$$C_1 = 2\hat{\mathbf{n}} \cdot \hat{\mathbf{K}} \left[2a - \frac{1+b}{b} \frac{\chi_0 + x^2}{1 - x^2} \right], \quad (3.2c)$$

$$C_0 = \frac{\chi_0^2 - 2\chi_0 a - x^2(1 + 2a)}{1 - x^2}, \quad (3.2d)$$

with a given by Eq. (2.20) and b , the asymmetry parameter, by

$$b = \frac{\hat{\mathbf{n}} \cdot \mathbf{K}}{\hat{\mathbf{n}} \cdot (\mathbf{K} + \mathbf{H})}. \quad (3.3a)$$

These equations are valid for arbitrary orientation of the

crystal surface. In the symmetric Bragg case the parameter b becomes

$$b = \frac{\sin\theta}{\sin\theta - 2\sin\theta_H}. \quad (3.3b)$$

Notice that the usual approximation of taking $b \simeq -1$ fails in the far tails of the Bragg peaks.

The four roots Δ_i ($i=1$ to 4) of the quartic Eq. (3.1) are shown in Fig. 5. In the symmetric Bragg case ($\hat{\mathbf{n}} = \hat{\mathbf{H}}$) the reflection symmetry of the dispersion surface can be exploited to calculate these roots exactly. As shown in the Appendix we obtain

$$\Delta_{1,4} = \Delta_0 - (A \pm B)^{1/2} \quad (3.4a)$$

and

$$\Delta_{2,3} = \Delta_0 + (A \pm B)^{1/2}, \quad (3.4b)$$

where

$$\Delta_0 = \sin\theta - \sin\theta_H, \quad (3.4c)$$

$$A = \sin^2\theta + \sin^2\theta_H + \frac{\chi_0 + x^2}{1 - x^2}, \quad (3.4d)$$

and

$$B = \left\{ \left[2\sin\theta\sin\theta_H + \frac{\chi_0 + x^2}{1 - x^2} \right]^2 - C_0 \right\}^{1/2}. \quad (3.4e)$$

The choice of signs in (3.4a) and (3.4b) should be made so that $\text{Re}\Delta_1 > \text{Re}\Delta_4$ and $\text{Re}\Delta_3 > \text{Re}\Delta_2$ (see Fig. 5).

For asymmetric Bragg cases the Δ_i can be easily calculated without neglecting the asymptotic sphericity of the dispersion surface if one notices that the roots Δ_3 and Δ_4 are sufficiently far away from the Bragg-peak region that the dispersion surface may be approximated by a sphere. These solutions are given in the Appendix.

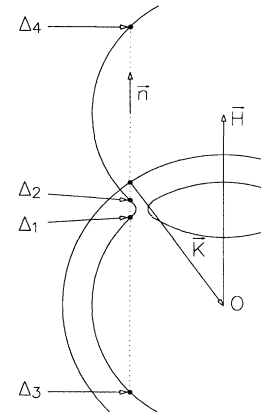


FIG. 5. The four roots Δ_i ($i=1$ to 4) of the quartic equation for the dispersion surface.

B. The boundary conditions

The boundary conditions used in Sec. II B neglected the distinction between electric \mathbf{E} and displacement \mathbf{D} fields. In the two-beam approximation the electric field in mode i ($i=1$ to 4), $\mathbf{E}^{(i)}$, is obtained from (2.1) and (2.10):

$$\mathbf{E}^{(i)}(t, \mathbf{r}) \simeq e^{-i\omega t} (\mathbf{E}_0^{(i)} e^{i\mathbf{k}_{i0} \cdot \mathbf{r}} + \mathbf{E}_H^{(i)} e^{i\mathbf{k}_{iH} \cdot \mathbf{r}}), \quad (3.5a)$$

where

$$\mathbf{E}_0^{(i)} = \mathbf{D}_0^{(i)} (1 - \chi_0) - \mathbf{D}_H^{(i)} \chi_H \quad (3.5b)$$

and

$$\mathbf{E}_H^{(i)} = \mathbf{D}_H^{(i)} (1 - \chi_0) - \mathbf{D}_0^{(i)} \chi_H. \quad (3.5c)$$

To be specific let us now consider the scattering by a semi-infinite crystal. In the usual approach (Sec. II B) only mode 1 is appreciably excited.¹⁻³ Modes 2 and 3 would only be excited if a second surface were present, and mode 4 is altogether neglected, which amounts to neglecting the Fresnel reflection of the diffracted beam as it leaves the crystal. The use of the correct electromagnetic boundary conditions requires that this fourth mode be included.

Close to the Bragg peak, the fields $\mathbf{E}_H^{(1)}$ and $\mathbf{D}_H^{(1)}$ of the dominant mode 1 are approximately equal because χ_0 and χ_H are small. In the far tail region, however, they are very different; the contribution of the second term in (3.5c) is comparable to that of the first and cannot be neglected. Thus,

$$\mathbf{E}_0^{(1)} \simeq \mathbf{D}_0^{(1)}, \quad (3.6a)$$

but

$$\mathbf{E}_H^{(1)} \simeq \mathbf{D}_H^{(1)} - \mathbf{D}_0^{(1)} \chi_H. \quad (3.6b)$$

For TE-polarized radiation, the use of the boundary conditions of tangential continuity of the Fourier components of the electric and magnetic fields (we assume nonmagnetic materials) leads to a rather simple result. There are reflected and diffracted waves. The amplitude reflection coefficient for the reflected wave is given by the appropriate Fresnel expression¹¹

$$r_R = \frac{K_n - k_{10n}}{k_{10n} - K_{Rn}}, \quad (3.7)$$

and, for the diffracted wave, we get

$$r_D = \left[\frac{K_n - K_{Rn}}{k_{10n} - K_{Rn}} \right] \left[r_A^{(1)} - \chi_H \right] \left[\frac{k_{1Hn} - k_{4Hn}}{K_{Dn} - k_{4Hn}} \right]. \quad (3.8)$$

Here \mathbf{K} , \mathbf{K}_D , and \mathbf{K}_R are the incident, diffracted, and reflected wave vectors, respectively, \mathbf{k}_{i0} and \mathbf{k}_{iH} are primary and diffracted wave vectors in mode $i=1$ or 4, the subscript n indicates the component along the normal $\hat{\mathbf{n}}$ to the crystal surface, and $r_A^{(1)}$ is the amplitude ratio (2.21) for mode 1. These expressions are valid for both the symmetric and nonsymmetric Bragg case.

Equation (3.7) differs from (2.8) only in the immediate vicinity of the Bragg peaks where the wave vector \mathbf{k}_1 lies

in the nontrivial part of the dispersion surface. Equation (3.8) also has a simple interpretation: The first factor on the right-hand side represents the transmission across the crystal surface into the crystal, from the incident \mathbf{E} amplitude to the amplitude of the zeroth component of mode 1 field $\mathbf{D}_0^{(1)}$. This factor is a Fresnel transmission coefficient; for nongrazing incidence it is very close to 1. The second factor represents the diffraction from the primary $\mathbf{D}_0^{(1)}$ to the diffracted $\mathbf{E}_H^{(1)}$; as discussed below Eq. (3.5) for low $r_A^{(1)}$, the extra term $-\chi_H$ is an important contribution. The third factor represents the transmission of the diffracted field $\mathbf{E}_H^{(1)}$ through the crystal surface out into the vacuum and, therefore, is essentially also a Fresnel transmission coefficient. The situation here is, however, rather peculiar in that this transmission coefficient may differ significantly from 1, in other words, the Fresnel reflection of the diffracted beam as it crosses the crystal-vacuum surface cannot be neglected. This is traced to the fact that in the far tail region the length of the wave vector \mathbf{k}_{1H} deviates from \mathbf{K} considerably (see Fig. 4) as if there were a large effective index of refraction.

In the symmetric Bragg case ($\hat{\mathbf{n}} = \mathbf{H}/H$) the reflected and diffracted beams coincide $\mathbf{K}_D = \mathbf{K}_R$ and the total reflectivity is the sum of the two contributions

$$R_{L2} = |r_R + r_D|^2. \quad (3.9)$$

Using Eq. (2.14), Eqs. (3.7) and (3.8) take the simpler form

$$r_R = \frac{\Delta_1}{2 \sin \theta - \Delta_1} \quad (3.10)$$

and

$$r_D = \left[\frac{2 \sin \theta}{2 \sin \theta - \Delta_1} \right] (r_A^{(1)} - \chi_H) \times \left[\frac{\Delta_1 - \Delta_4}{2 \sin \theta - 2 \sin \theta_H - \Delta_4} \right]. \quad (3.11)$$

C. The kinematical and improved dynamical results compared

Let us return to the specific diffraction example considered in Sec. II C. The reflectivity calculated according to the kinematical and the improved dynamical theories, including the contribution of the Fresnel reflectivity, is given by Eqs. (2.7), (2.8), and (3.9)–(3.11), respectively, and is shown in Fig. 6.

We see that the kinematical result (curve labeled $\text{KT} + F$) agrees with the improved Laue dynamical result (curve labeled $\text{LT2} + F$) over the *entire* angular range between the zeroth order (the total external reflection region) and the first order (the 111 reflection). As expected, they differ only at the (111) Bragg peak. In this region of large R the improved dynamical result coincides with the usual Laue theory [shown in Fig. 3(a)] and, as discussed earlier, the kinematical result is wrong.

This agreement between the improved dynamical and the kinematical theory in the far tail region can be

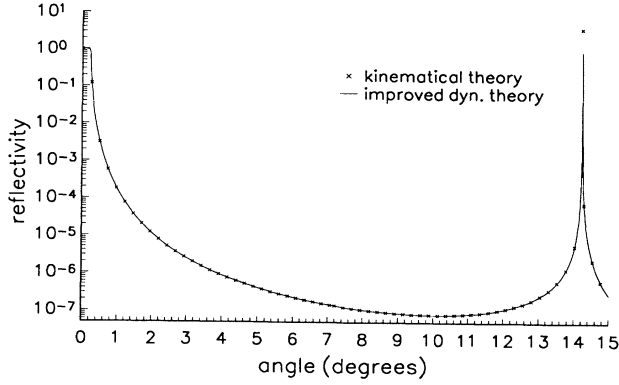


FIG. 6. The reflectivity of the ideally terminated silicon crystal to $\text{CuK}\alpha$ radiation including the (111) Bragg reflection and the contribution due to the Fresnel reflectivity, according to the kinematical (KT+F) and the improved Laue dynamical theories (LT2+F). The improved dynamical theory agrees with the kinematical theory everywhere except at the Bragg peak where the kinematical theory is known to fail. A blowup of the Bragg-peak region at 14.2° is identical to Fig. 3(a).

demonstrated analytically. Note that sufficiently far away from the resonance region the dispersion surface is very close to spherical (see Fig. 5). To calculate Δ_1 , we set $\xi_0 \approx 0$ in Eq. (2.12a) and combine with (2.14) to get, in the symmetric Bragg case

$$\Delta_1 \approx \sin\theta - \sin\bar{\theta}. \quad (3.12)$$

Similarly, setting $\xi_H \approx 0$ in Eq. (2.12b) and using (2.14) we get

$$\Delta_4 \approx \sin\theta - \sin\bar{\theta} - 2\sin\theta_H. \quad (3.13)$$

The amplitude ratio $r_A^{(1)}$ is obtained from (2.12b), (2.14), and (3.12),

$$r_A^{(1)} = \frac{\chi_H}{2\xi_H} \approx \chi_H \left\{ \frac{1 + \chi_0}{4\sin\theta_H(\sin\theta_H - \sin\bar{\theta})} + 1 \right\}. \quad (3.14)$$

Substituting (3.12)–(3.14) into (3.10) and (3.11) we obtain the kinematical expressions (2.7) and (2.8) to leading order in χ , as desired.

IV. FINAL REMARKS AND CONCLUSIONS

We have shown that the expectation that the kinematical and the Laue dynamical theories of x-ray diffraction give equivalent results for the weak scattered intensities in the far tails of the Bragg peaks is justified provided some approximations employed in the dynamical calculation are improved. Better approximations for both the shape of the dispersion surface and the boundary conditions are required: One needs to take into account the asymptotic sphericity of the dispersion surface and the difference between electric and displacement fields. This results in a nontrivial transmission coefficient for the diffracted electric field as it leaves the crystal.

Our approach has relied on analytical rather than numerical calculations. Rather than scanning reciprocal space across the truncation rods (as in Ref. 10), the calcu-

lations described here refer to scanning along the truncation rods, which is more directly relevant for some experiments.⁷ In fact, by explicitly showing the equivalence of kinematical and dynamical results this work provides additional theoretical support for the kinematical approach adopted in Ref. 7.

ACKNOWLEDGMENTS

Many useful conversations with R. Deslattes, T. Jach, C. Chantler, and E. Vlieg are gratefully acknowledged. This work was partially supported by Grant No. AFOSR 88-0018 and by a grant from Defense Advanced Research Project Agency (DARPA) Microelectronics Technology Office.

APPENDIX: SOLUTIONS OF THE QUARTIC EQUATION FOR THE DISPERSION SURFACE

The four roots Δ_i ($i=1$ to 4) of the quartic equation for the dispersion surface satisfy

$$\sum_i \Delta_i = -C_3, \quad (A1)$$

$$\sum_{i \neq j} \Delta_i \Delta_j = C_2, \quad (A2)$$

$$\prod_i \Delta_i = C_0. \quad (A3)$$

In the symmetric Bragg case the reflection symmetry of the dispersion surface implies (see Fig. 5) that the Δ_i are of the form

$$\Delta_{1,4} = \Delta_0 - \Delta_{a,b} \quad (A4a)$$

and

$$\Delta_{2,3} = \Delta_0 + \Delta_{a,b}. \quad (A4b)$$

Substituting into (A1) and using (3.2a) and (3.3b), we see that Δ_0 is given by (3.4c). Substituting further into (A2) and (A3), we obtain a quadratic equation for $\Delta_{a,b}$, which leads to the desired solution (3.4).

In an asymmetric geometry where $\hat{\mathbf{n}}$ is not parallel to \mathbf{H} and Eqs. (A4) are not valid, one may still obtain an approximation that takes the correct asymptotic sphericity into account by noting that the roots Δ_3 and Δ_4 are located sufficiently far away from the resonance region that the dispersion surface is very close to spherical (see Fig. 5). Analytically this is expressed by setting $\xi_0 \approx 0$ in Eq. (2.12a). Combining this with (2.14) we get

$$\Delta_3 \approx \Delta'_3 = -\hat{\mathbf{n}} \cdot \hat{\mathbf{K}} + [(\hat{\mathbf{n}} \cdot \hat{\mathbf{K}})^2 + \chi_0]^{1/2}. \quad (A5)$$

Similarly, setting $\xi_H \approx 0$ in Eq. (2.12b) and using (2.14) we get

$$\Delta_4 \approx \Delta'_4 = -\frac{\hat{\mathbf{n}} \cdot \hat{\mathbf{K}}}{b} - \left[\left(\frac{\hat{\mathbf{n}} \cdot \hat{\mathbf{K}}}{b} \right)^2 - 2a + \chi_0 \right]^{1/2}. \quad (A6)$$

Substituting into (A1) and (A3) we get the desired solutions,

$$\Delta_{1,2} = -\frac{1}{2}(C_3 + \Delta'_3 + \Delta'_4) \pm \left[\frac{1}{4}(C_3 + \Delta'_3 + \Delta'_4)^2 - \frac{C_0}{\Delta'_3 \Delta'_4} \right]^{1/2}. \quad (A7)$$

*Present address: Department of Physics, SUNY Albany, Albany, NY 12222.

¹R. W. James, *The Optical Principles of the Diffraction of X Rays* (G. Bell, London, 1958).

²W. H. Zachariasen, *Theory of X-Ray Diffraction in Crystals* (Dover, New York, 1967).

³N. Kato, *X-Ray Diffraction*, edited by L. Azàroff (McGraw-Hill, New York, 1974), Chaps. 3 and 4.

⁴B. E. Warren, *X-Ray Diffraction* (Dover, New York, 1990).

⁵S. Kishino, and K. Kohra, *Jpn. J. Appl. Phys.* **10**, 551 (1971); T. Bedyńska, *Phys. Status Solidi A* **19**, 365 (1973); **25**, 405 (1974); J. Härtwig, *ibid.* **37**, 417 (1976); **42**, 495 (1977); A. M. Afanas'ev and M. K. Melkonyan, *Acta Crystallogr. Sect. A* **39**, 207 (1983); T. Jach, P. L. Cowan, Q. Shen, and M. Bedzyk, *Phys. Rev. B* **39**, 5739 (1989).

⁶O. Brümmer, H. Hoche, and J. Nieber, *Phys. Status Solidi A* **53**, 565 (1979); A. Caticha and S. Caticha-Ellis, *Phys. Rev. B*

25, 971 (1982).

⁷S. R. Andrews and R. A. Cowley, *J. Phys. C* **18**, 6427 (1985); I. K. Robinson, *Phys. Rev. B* **33**, 3830 (1986); I. K. Robinson, R. T. Tung, and R. Feidenhans'l, *ibid.* **38**, 3632 (1988); D. Gibbs *et al.*, *Phys. Rev. D* **38**, 7303 (1988); S. G. Mochrie, *Phys. Rev. Lett.* **64**, 2925 (1990).

⁸J. H. Underwood and T. W. Barbee, *Appl. Opt.* **20**, 3027 (1981); P. Lee, *Opt. Commun.* **37**, 159 (1981); B. L. Henke *et al.*, *Opt. Eng.* **25**, 937 (1986); W. J. Bartels *et al.*, *Acta Crystallogr. Sect. A* **42**, 539 (1986); P. G. Harper and S. K. Ramchurn, *Appl. Opt.* **26**, 713 (1987); E. Spiller, *Rev. Phys. Appl.* **23**, 1687 (1988); B. Pardo *et al.*, *J. Opt.* **22**, 141 (1991).

⁹G. H. Vineyard, *Phys. Rev. B* **26**, 4146 (1982).

¹⁰R. Colella, *Phys. Rev. B* **43**, 13827 (1991).

¹¹M. Born and E. Wolf, *Principles of Optics* (Pergamon, New York, 1975).